

Searching for the Sources Responsible for Cosmic Reionization: Probing the Redshift Range $7 < z < 10$ and Beyond

Daniel P. Stark¹ & Richard S. Ellis¹

¹*Dept. of Astronomy, California Institute of Technology, Pasadena CA 91125
E-mail: dps@astro.caltech.edu*

Abstract

We review recent observations that suggest that the global star formation rate density of UV-bright galaxies is declining monotonically with redshift over $3 < z < 7$ and illustrate the challenges that a continuation of this decline poses in explaining the assembled stellar mass in several $z \sim 6$ galaxies deduced from recent Spitzer data. A plausible conclusion is a vigorous period of yet earlier star formation. Prior to JWST and TMT, strong lensing offers a unique probe of the extent of this earlier activity. We discuss the first results of a blind spectroscopic survey of 10 lensing clusters for $8.5 < z < 10$ Ly α emitters using NIRSPEC on Keck. We demonstrate this survey is achieving an (unlensed) sensitivity equivalent to a star formation rate of $0.1 M_{\odot} \text{ yr}^{-1}$. A companion survey, now beginning with HST and Spitzer, will target lensed z and J -band dropouts and probe a $\simeq 1 \text{ arcmin}^2$ region 1 magnitude deeper than the UDF/NICMOS observations. In combination, both surveys will provide the first constraints on the contribution of early, low luminosity, sources to cosmic reionization.

Key words: cosmology:observations, galaxies: high redshift, gravitational lensing

1 Introduction

The reionization of neutral hydrogen which rendered the Universe transparent to UV photons and thereby terminated the so-called ‘dark ages’ was a landmark event in cosmic history. Determining the nature, abundance and redshift distribution of the sources responsible for this important transition represents the current frontier in studies of the first galactic systems.

Recent developments strongly motivate a systematic search for star-forming sources beyond $z \simeq 7$. The WMAP temperature-polarization cross correlation

signal on large angular scales (1) implies scattering of microwave photons by free electrons from ionizing sources at $z \simeq 10-12$ (2). The abundance of luminous UV-emitting i -band (4), z -band, and J -band (5),(6) ‘drop-outs’ in the Hubble Ultra Deep Field at $z \simeq 6, 7$ and 10 respectively, suggests a surprisingly continuous decline in the comoving density of emerging UV photons to $z=10$. The luminosity density of these UV-bright sources seems insufficient to reionize the universe unless non-standard initial mass functions (3) or very steep faint end-slopes for the luminosity function (7) are invoked. More likely is the possibility of an intense earlier period of star formation. Meanwhile, Spitzer observations have uncovered a population of very massive ($M_{stellar} \sim 10^{10} - 10^{11} M_{\odot}$) galaxies with well-established stellar populations (11), (19), (20), (24). Given the decline in the star formation rate density of UV-emitters, the presence of this massive population requires explanation. While extinction and cosmic variance likely play a role in the apparent discrepancy, an earlier period of vigorous star formation may have contributed significantly to buildup these massive galaxies as well as producing a substantial fraction of the photons required for reionization.

Finding this early population is one of the primary goals of observational cosmology. With current facilities, traditional search methods are poorly equipped to search beyond $z \simeq 7$. Even with HST and 8-10 meter class telescopes, continuum (‘drop-out’) and narrow-band imaging Lyman α searches only probe the most luminous, rare, sources at these redshifts; the contribution to the reionization flux from these sources may well be small. The study of lower luminosity sources rendered visible by the strong gravitational lensing induced by clusters with well-constrained mass models can greatly assist in this work. A typical lensing cluster magnifies sources by $\times 5-10$ over 1 arcmin^2 for sources at $z > 7$. Moreover, on the critical line, faint signals are boosted $> \times 30$ and spectroscopy and more detailed studies are often feasible at otherwise impossible (unlensed) limits. For several objects recently located via this technique (8), (9), (10), stellar continuum slopes, Ly α profiles and star formation rates have been determined for sources whose intrinsic flux is close to the UDF limit, $I_{AB} \simeq 30$. Perhaps most remarkably, such sources have been magnified so as to become accessible by Spitzer (11) yielding luminosity-weighted ages.

Until the era of TMT/JWST, scanning the critical lines of massive clusters provides possibly the only reliable means of estimating the abundance of low luminosity star forming sources in the $7 < z < 10$ interval with minimal contamination. In these proceedings, we discuss two such surveys: in §4, we report on the progress of a Keck spectroscopic survey along cluster critical lines for Ly α emitters at $z > 8$, and in §5 we present a new 110 orbit Hubble imaging survey for lensed low-luminosity galaxies at $z \sim 7-10$.

2 Evidence for a Declining Star Formation Rate

Optical and near-infrared imaging with the Hubble Space Telescope have tentatively provided the first limits on the visible star formation activity in the era $6 \lesssim z \lesssim 10$. Galaxies are identified at these redshifts by extending the Lyman-break technique (12), (13) to $z > 6$, and their star formation rates are estimated by measuring their rest-frame ultraviolet emission, which is dominated by young massive stars.

The abundance of $z \sim 6$ galaxies (identified as i' -dropouts) has been calculated in the 400 arcmin² GOODS-North and GOODS-South fields down to $z_{AB} < 25.6$ (15),(16), in ACS parallel observations covering 10 arcmin² down to $z_{AB} < 28.3$ (17), in ACS GTO fields spanning 46 arcmin² reaching down to $z_{AB} < 27.3$ (18), in the ACS parallels to the NICMOS UDF observations which span 21 arcmin² down to $z_{AB} < 28.1$, and in the 11.3 arcmin² UDF down to $z_{AB} < 28.5$ (4) and down to $z_{AB} < 29.2$ (7). In addition, the exceptional depth of the HST NICMOS images of the UDF allows galaxies at $z \sim 7$ and $z \sim 10$ to be identified as z -drops and J-drops, respectively (5), (6).

The general consensus emerging from these studies is that the apparent star formation rate density, uncorrected for extinction (integrated down to $L_{UV} > 0.1 L_{z=3}^*$) is ~ 3 -6 times less at $z \sim 6$ than at $z \sim 3$ and continues to decline out to $z \sim 10$ (integrated down to $L_{UV} > 0.3 L_{z=3}^*$) (Fig 1). The declining star formation rate poses a challenge for models suggesting star-forming galaxies at $z \sim 6$ reionized the Universe. The low-abundance of high- z dropouts can be reconciled with such models if the galaxies have low metallicity or a non-standard initial mass function (3), or if the UV luminosity function has a very steep faint-end slope (7), such that the bulk of ionizing photons are released by intrinsically faint galaxies that lie below the 5σ sensitivity limit of the UDF. Alternatively, the bulk of reionization may occur at yet earlier times, requiring the presence of a significant abundance of objects at $z \gg 6$, or conceivably reionization was not accomplished by young star-forming galaxies.

3 The Crucial Role of Spitzer

Detecting light from the most distant galaxies known in the universe has been one of the most remarkable and important feats of the IRAC instrument on-board the 85 cm Spitzer Space Telescope. The IRAC filters at 3.6-8.0 μm probe the rest-frame optical and near-infrared at $z > 6$, providing the first glimpse of light from established stellar populations of galaxies at such high redshift. Combining these data with deep broadband optical photometry from HST and 8-10 meter class ground based telescopes, spectral energy distributions

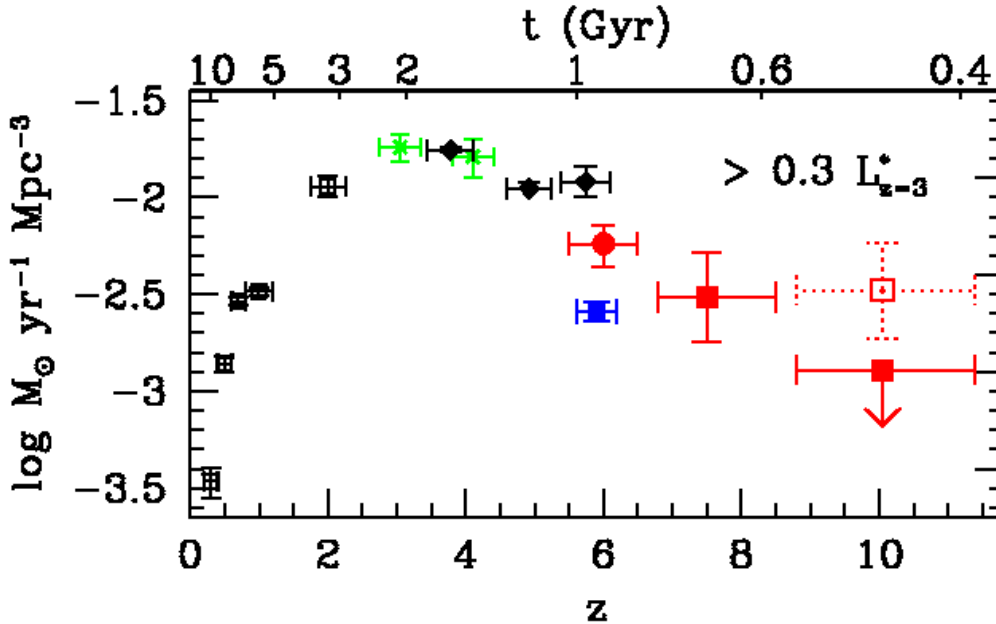


Fig. 1. The co-moving volume density of luminous UV emitting galaxies located via the ‘drop out’ technique with recent UDF estimates from (4) and (5), (6), uncorrected for extinction, as presented in (6). The integrated abundance to $z \simeq 10$, while uncertain, appears to be insufficient for cosmic reionization. Possible explanations include an abundant population of lower luminosity sources or vagaries of cosmic variance in the small UDF field. Our surveys (§4 and §5) test both hypotheses.

(SEDs) can be constructed and compared with population synthesis models to constrain the age, star formation history, and stellar mass of galaxies at $z \sim 6-7$. In providing the opportunity to characterize the stellar mass density at $z \sim 6-7$, Spitzer allows the first constraints to be placed on the star formation rate density integrated over the first 800 Myr of the Universe.

The first demonstration of an established stellar population at high redshift was via the strongly-lensed $z \sim 6.8$ galaxy in Abell 2218 (11). The initial identification of this triply-lensed source was based on detections in the F814W, F850LP, and F160W HST filters ($0.801 \mu\text{m}$, $0.905 \mu\text{m}$, and $1.612 \mu\text{m}$ respectively). Subsequent detections were made at $3.6 \mu\text{m}$ and $4.5 \mu\text{m}$ with Spitzer for one of the components of the lensed system and at $1.1 \mu\text{m}$ with HST for two of the three lensed images. With the new photometric data, the galaxy’s SED was constructed and compared to model SEDs generated with the GALAXEV population synthesis code (14). Best-fit SEDs of this source (Fig 2) are obtained by varying the galaxy age and redshift for a given star formation history and minimizing χ^2 . The results suggest that the age of the galaxy is between 40-450 Myr, corresponding to a formation redshift of $z_f \sim 7 - 12$. In each case the best-fit age of the galaxy is greater than the assumed e-folding star formation timescale, indicating that the galaxy would have been

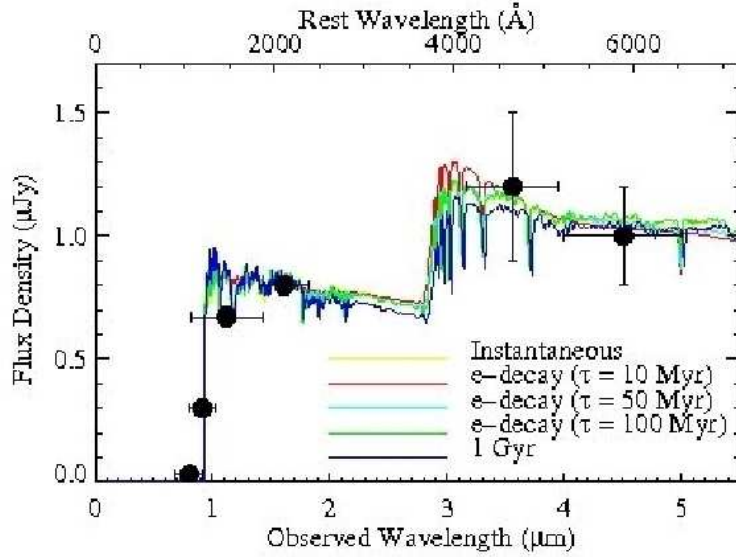


Fig. 2. SED of the $z \simeq 6.8$ lensed source in Figure 2 from (11). The combination of Spitzer and HST photometry spans the rest-frame UV to optical determining the luminosity-weighted stellar age ($\simeq 100$ Myr) suggesting a credible source of UV photons since $z \simeq 10$.

more luminous in the ultraviolet at earlier times during its active star-forming phase. Given the small survey area required for its discovery, such sources may have a reasonably high surface density suggesting that a population of intense star-forming galaxies ($10\text{-}100 M_{\odot} \text{ yr}^{-1}$) may be very common at $z > 7$, contributing significantly to the UV photon budget required for reionization.

The key feature which makes the lensed source in Abell 2218 of great diagnostic value is the Balmer break observed between the NICMOS F160W and $3.6 \mu\text{m}$ bands; this indicates an age $\gtrsim 100$ Myr and a declining star formation rate. Similar signatures have been subsequently seen in more massive systems at $z \sim 6\text{-}7$ ($M_{\text{stellar}} \simeq 10^{10} M_{\odot}$). The SEDs of four *i*-drops in GOODS-South, spectroscopically confirmed by us at Keck, are constructed in (19). Two of the four galaxies have robust Spitzer detections at $3.6 \mu\text{m}$ and $4.5 \mu\text{m}$. Comparisons to population synthesis models (14) yield stellar mass estimates of $2\text{-}4 \times 10^{10} M_{\odot}$ and ages between 250-650 Myr ($z_f \sim 7.5\text{-}13.5$). Very recently, similarly massive systems have been presented for a larger sample in the UDF (24). In order to build up such a stellar mass, the average SFR at earlier times must be greater than that observed at $z \simeq 6$.

Perhaps the most intriguing high-redshift object studied with Spitzer is a $z \sim 7$ galaxy in the Hubble UDF with a stellar mass claimed to exceed $10^{11} M_{\odot}$ (20). The high-redshift interpretation is favored as a result of the strong break in flux between the K-band and $3.6 \mu\text{m}$ (interpreted as the rest-frame 3646 \AA Balmer break) and the null detection in deepest optical broadband images ever obtained (3σ detection limit of 31.5 in AB mags over a 1.5 arcsec aperture

in the combined BViz ACS images of the UDF). The best-fitting population synthesis models have very little dust extinction and ages of several hundred Myr, placing the epoch of formation of the bulk of this galaxy's stellar mass at $z_f > 10$. Even if star formation occurred in several sub-galactic units which subsequently merged, remarkably high star formation rates ($> 1000 M_\odot \text{ yr}^{-1}$) may be required to assemble the stellar mass of this system by $z \sim 7$.

4 A Systematic Survey for Strongly-Lensed Ly α emitters at $z > 8$

4.1 Survey Strategy

The above discussion provides a clear motivation for searching for earlier activity and, prior to JWST and TMT, lensing offers a reasonable prospect of making some progress. We have undertaken a Keck spectroscopic survey for strongly-lensed star-forming sources at $z > 8$. Using NIRSPEC in the J-band (sensitive to Ly α emitters at $8.5 < z < 10.2$), we scan the critical lines of ~ 10 lensing clusters. By only observing along regions of very high magnification ($\times 30$ across most of the slit), we become sensitive to feeble sources producing stars with rates as low as $\sim 0.1 M_\odot \text{ yr}^{-1}$. All clusters used in our survey have spectroscopically-confirmed redshifts for a number of multiple images and arcs, allowing for the derivation of detailed magnification maps for high-redshift sources (Figure 3).

Redshift identification of candidates is aided by several factors. The cluster lensing model constrains the redshift of any strongly-lensed source for which multiple images are detected via the observed image flux ratios and positions. In addition, by using NIRSPEC to search for Ly α emitters in the same clusters studied with LRIS on Keck in the optical (9), we are able to correlate emission lines seen in the J band with existing optical spectroscopic data to clarify possible interlopers which are not multiply-imaged. Further, deep HST optical broadband imaging is available for all of our clusters. Ly α emitters at $z > 8$ should be virtually invisible in the optical due to IGM absorption. Hence, the presence of optical flux spatially coincident with a candidate $z > 8$ Ly α emitter would indicate that the candidate is at low-redshift.

4.2 Results and Discussion

Twelve Keck nights have been allocated for this project. Nine nights have been completed thus far, of which 5.5 have been clear. During these 5.5 nights, 31 slit positions were mapped toward seven clusters with an average integration

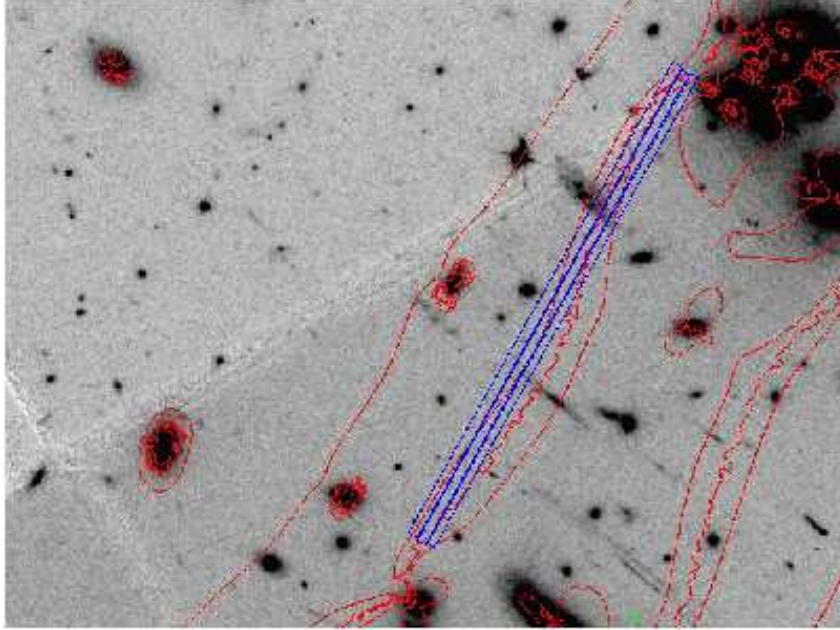


Fig. 3. The Keck NIRSPEC blind survey: slit positions observed toward Abell 68. Amplification contours ($\times 5,30$) are overlaid on the HST WFPC2 R-band image. The magnification appropriate for $z > 6$ background sources is > 30 for the entire extent of each of the three slit positions.

time of 1.4 hours each. Each slit position consists of 6 to 9 ten minute exposures that were dithered parallel to the length of the slit.

Spectra are flat-fielded and sky-subtracted with IDL routines following the optimal spectroscopic reduction techniques presented in (21). We determine the pointing of each exposure on the sky by registering images from the NIRSPEC slit-viewing camera to HST images of the same field. Offsets between exposures of a given slit position are calculated from the registered slit viewing camera images, and the spectra are subsequently shifted and combined. In Figure 4, we present the reduced final two-dimensional spectra of three slit position toward Abell 68.

The sky-subtracted two-dimensional spectra were independently inspected for candidates by the authors. A catalog of fifteen possible high- z Ly α emitters was constructed and cross-checked with deep HST optical and ground-based near-IR images for corresponding broadband emission. Most candidates lack convincing emission in the ground-based near-IR broadband images. Final confirmation of these sources awaits deeper HST near-IR imaging (see § 5).

Our limiting Ly α line flux is defined to be the signal in an aperture 1.0 arcsec by 12 \AA that is five times the root-mean-square fluctuation in an aperture of that size. The spatial dimension was chosen to be roughly twice the typical seeing disk of the observations, and the spectral dimension was chosen to match the typical Ly α line width of high-redshift galaxies, $\sim 300 \text{ km s}^{-1}$

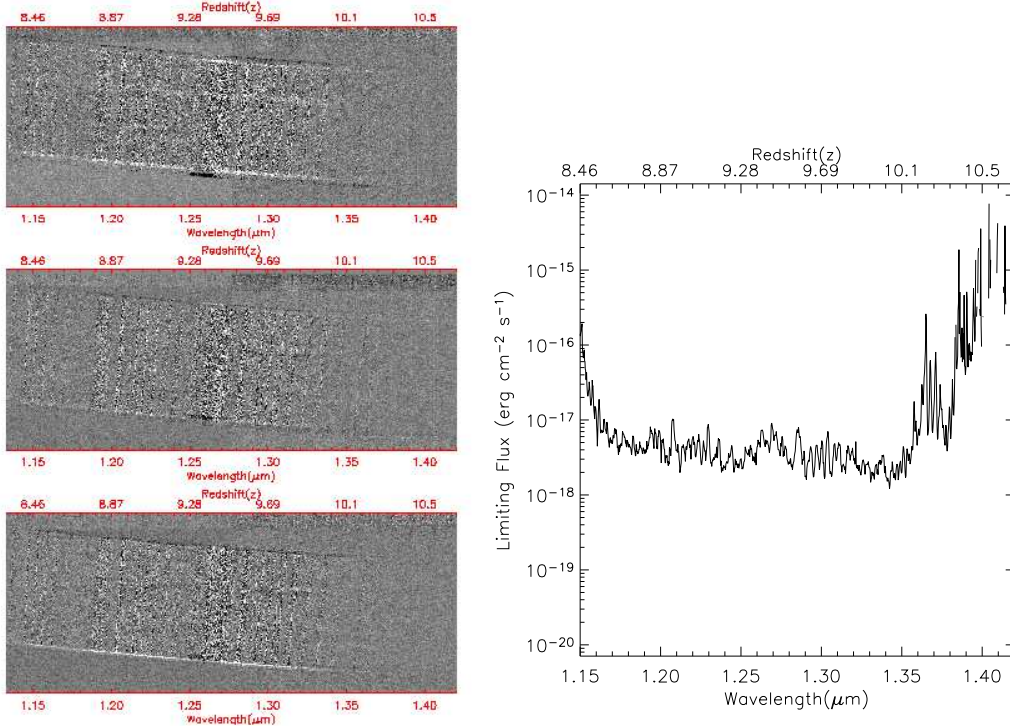


Fig. 4. Left: Reduced two-dimensional spectra of three slit positions toward Abell 68. A faint continuum trace from a foreground spiral galaxy is apparent in each of the three slit positions. Right: The minimum detectable flux (5σ) for an observed Ly α line as a function of wavelength (and redshift) from a 1.5 hour exposure with NIRSPEC. Depending on the local magnification, this observed limit of $<10^{-17}$ erg cm $^{-2}$ s $^{-1}$ corresponds to a star formation rate of $\simeq 0.03$ - $0.1 M_{\odot}$ yr $^{-1}$.

(9). Typical 5σ limiting line fluxes between OH lines range between $f_{\alpha}=3 \times 10^{-18}$ erg cm $^{-2}$ s $^{-1}$ and 1×10^{-17} erg cm $^{-2}$ s $^{-1}$ (Figure 4). The corresponding characteristic limiting Ly α line luminosity of our survey is $\sim 10^{41}$ erg s $^{-1}$ after correction for the typical $\times 30$ magnification. Converting this line luminosity to a star formation rate, assuming $1 M_{\odot}$ yr $^{-1}$ of star formation produces 10^{42} erg s $^{-1}$ of luminosity in the Ly α line (22), we find the typical unlensed limiting star formation rate is $\sim 0.1 M_{\odot}$ yr $^{-1}$.

To obtain a rough estimate of the surface density of galaxies we would expect to find in our survey if low-luminosity galaxies dominate the reionization process, we consider two scenarios: 1) an extended reionization period ($z=20$ to $z=7$, $\Delta t=575$ Myr) with a moderate ionizing photon escape fraction ($f_c=0.5$) and 2) a relatively quick reionization period ($z=10$ to $z=7$, $\Delta t=300$ Myr) with a lower ionizing photon escape fraction ($f_c=0.1$). With these assumptions, we find that the surface density of sources in our survey must exceed 200 arcmin $^{-2}$ for the extended reionization case and 2000 arcmin $^{-2}$ for the abrupt reionization scenario (Figure 5). Given our expected survey area of 0.015 arcmin 2 (unlensed), upon completion of our survey we should detect several sources under a range of reionization scenarios.

We note that realistically, galaxies of all luminosities contribute to the reionization process. If the number density of galaxies continues to rise steeply toward star formation rates below the limiting rate of our survey, the number density of star-forming sources required for reionization is lower than we estimate above. We consider this possibility in more detail in a future paper (Stark et al. 2005, in prep).

At the time of writing about half of our survey data has been analyzed suggesting that the abundance of galaxies at these early times is not significantly greater than that required for reionization under the assumptions mentioned above; however, it is clear from Figure 5 that our ability to detect reionization sources and provide meaningful constraints on the contribution of intrinsically faint galaxies to reionization at $z > 8$ will be significantly enhanced upon completion of our survey.

Figure 5 also provides an opportunity for us to consider the challenge of explaining the surface density of massive stellar systems being found by Spitzer at $z \sim 6$ (11), (19), (24). For each of the surveys (marked), we estimate the lower limit to the mass density from the sources so far seen and infer an equivalent lower limit to the (constant) star formation rate density required over the interval $6 < z < 20$ to account for this mass. Not only are the estimates close to being adequate for reionization but, if the decline in Fig. 1 is correct, the presence of a few massive galaxies in the small fields so far surveyed already suggests the need for a very short intense period of activity at high redshift.

5 An HST+Spitzer Search for Strongly-Lensed $z=7-10$ Galaxies

To complement the Ly α search, we have recently begun a HST large program (110 orbits) that will survey six cluster fields totaling 10 arcmin² in three wide-band filters (ACS-WFC/F850LP, NIC3/F110W, NIC3/F160W) to characterize the faint, star-forming galaxies responsible for the completion of cosmic reionization at $z > 7$. We achieve the necessary depth by boosting the sensitivity of HST with magnification from powerful lensing clusters at intermediate redshifts (Figure 6).

We will select $z > 7$ sources using well-established color-selection techniques based on the neutral hydrogen break at rest-frame Lyman α (e.g., (18), (5); (16)). Incorporating the lensing magnification, more than half our survey area will reach unlensed star-formation rates of $< 1M_{\odot} \text{ yr}^{-1}$ (for nominal source assumptions), i.e. better than the NICMOS UDF survey (5). Although lensing reduces the surveyed volume by the linear magnification, our total volume at UDF depths is still almost 25% of the NICMOS UDF field. Moreover, 2.5 arcmin² is imaged more than one magnitude deeper in many sightlines and

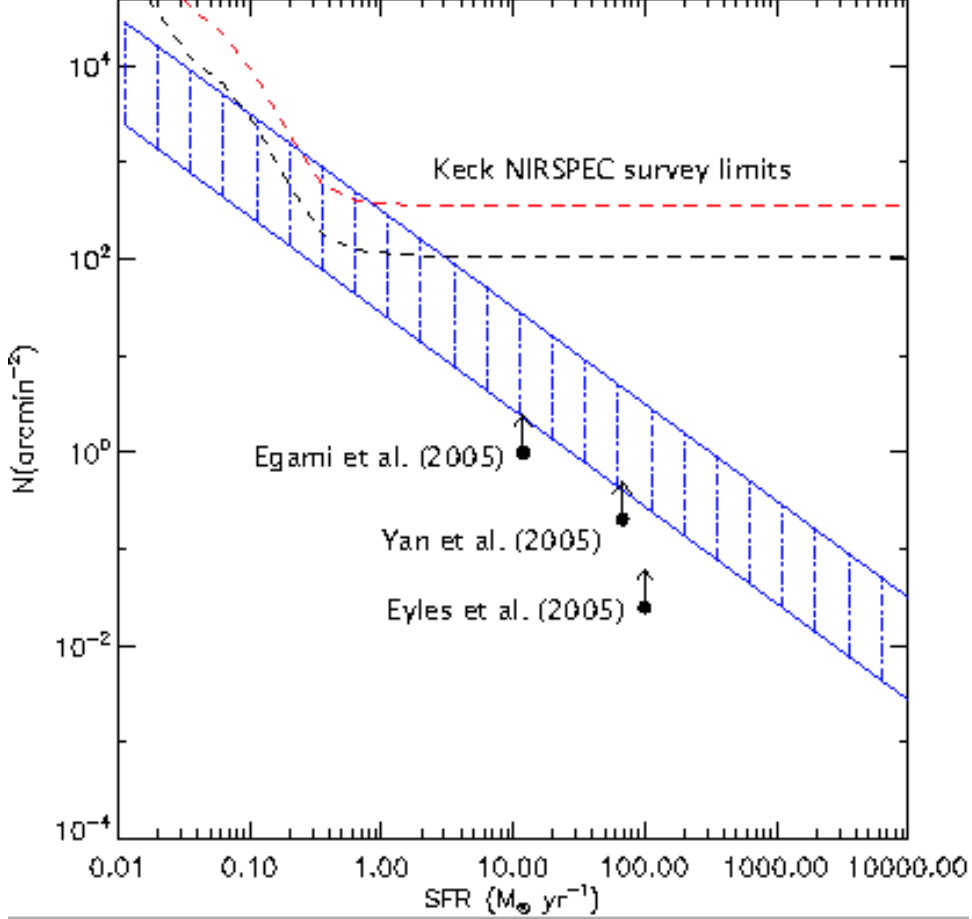


Fig. 5. Estimates of the surface density of sources necessary for cosmic reionization over $7 < z < 10$. The blue hatched area represents the likely range for various scenarios; the lower bound represents an extended phase ($7 < z < 20$) and moderate ionizing photon escape fraction ($f_c=0.5$) and the upper bound represents a rapid phase ($7 < z < 10$) and a low ionizing photon escape fraction ($f_c=0.1$). Dashed curves illustrate our sensitivity limits (5σ) to the surface density of star-forming sources using our present analyzed data (top curve) and that for the completed survey (bottom curve). A lower limit to the abundance of star-forming galaxies required to build the $z \simeq 6$ massive galaxies described in (11), (19), (24) over the period $7 < z < 20$ is also displayed. Taken together with Fig. 1 these massive systems implies a very early period of intense activity sufficient for cosmic reionization.

the fidelity of our sample will be assured by the well-understood geometrical effects of lensing.

Both observational evidence (7) and theoretical conjecture (23) suggest the counts of faint $z > 7$ galaxies should be steeply rising at the UDF limit. Clearly at $z \simeq 7$ only the most luminous galaxies are presently detectable (5). Extrapolating one magnitude deeper (Fig. 7) suggests we will reach a surface density of 11 arcmin^{-2} and find at least 5 sources fainter than the UDF limit, approaching the minimal luminosity density necessary for reionization.

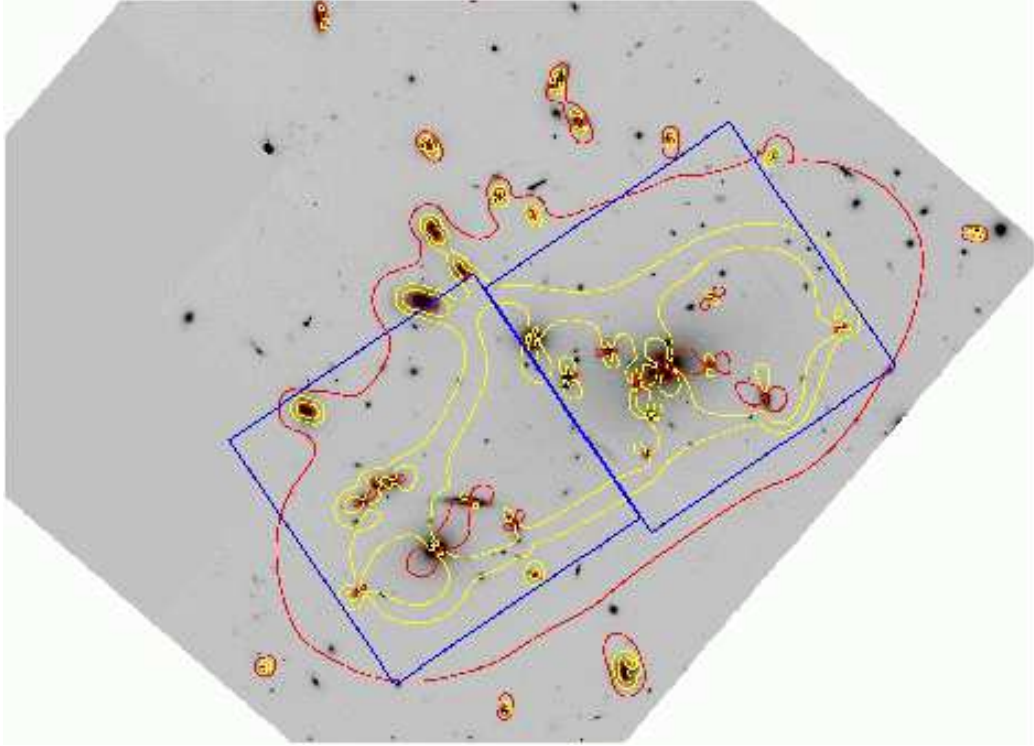


Fig. 6. Deployment of HST NICMOS images (squares) for Abell 2219 - one of the target clusters. The outer curve defines the area within which, as a result of lensing magnification, the proposed survey will go deeper than the NICMOS UDF campaign. The regions inside the yellow curves represent areas of extreme ($\times 30$) magnification.

A major bonus of our program is that magnified sources are brought within reach of the Spitzer Space Telescope. All of our target clusters have been imaged by IRAC at 3.6 and 4.5 μm , to the same $5\text{-}\sigma$ point-source sensitivity of 1 μJy as Abell 2218. The extended wavelength baseline offered by the combination of HST and Spitzer can uniquely characterize physical properties (age, star formation history) for $z \simeq 7$ objects that would be too faint to otherwise be studied (11). By analogy with our analysis in Abell 2218, we can verify whether long-lived sources are the norm at $z \simeq 6\text{-}7$. Tantalizingly, the combination of IRAC and NICMOS photometry also offers the prospect of searching for their more distant ancestors, $z \simeq 8\text{-}10$, via dropouts selected at the F110W/F160W boundary.

References

- [1] Kogut, A et al, 2003, ApJS **148**, 161
- [2] Fugugita, M & Kawasaki, M MNRAS **343**, L25 (2003)
- [3] Stiavelli, M., Fall, M.S., Panagia, N. ApJ, **610** L1, (2004b)

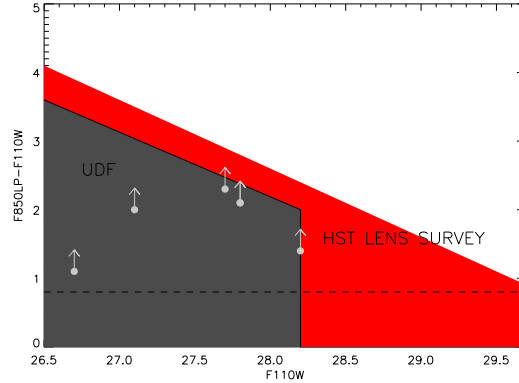


Fig. 7. Comparison of proposed sensitivity limits for the HST NICMOS/Spitzer deep survey (assuming a typical lens magnification of 30) with those of (5) in the UDF (grey region). The $z \sim 7$ sources identified by (5) are plotted as light grey limits. We will therefore explore new parameter space that was inaccessible to the UDF. Specifically, we will achieve more stringent limits on F850LP-F110W colors and be sensitive to sources down to $F110W \simeq 30$.

- [4] Bunker, A., Stanway, E., Ellis, R., McMahon, R.G., MNRAS **355**, 374 (2004).
- [5] Bouwens, R. et al. ApJ **616**, L79 (2004b).
- [6] Bouwens, R., Illingworth, G.D., Thompson, R.I., Franx, M. ApJ **624**, L5 (2005).
- [7] Yan, H, & Windhorst, R., ApJ, **612**, L93 (2004)
- [8] Ellis, R.S., Santos, M.R., Kneib, J.P., & Kuijken, K. ApJ **560** L119 (2004)
- [9] Santos, M. , Ellis, R., Kneib, J.P., ApJ, **606** 683, (2004)
- [10] Kneib, J-P., Ellis, R.S., Santos, M.R., Richard, J. ApJ **607** 697, (2004)
- [11] Egami, E. et al. ApJ **618**, L5 (2005)
- [12] Steidel, C., Pettini, M., & Hamilton, D., **110** 2519 (1995)
- [13] Steidel, C. Giavalisco M., Pettini, M., Dickinson, M., Adelberger K.L. ApJ **462** L17 (1996)
- [14] Bruzual, G. & Charlot, S. MNRAS **344**, 1000. (2003)
- [15] Stanway, E., et al. ApJ, **342** 439 (2003)
- [16] Stanway, E., et al. ApJ, **607** 704 (2004)
- [17] Yan, H, & Windhorst, R., & Cohen, S., ApJ, **585**, L93 (2003)
- [18] Bouwens, R., et al. ApJ **606**, L25 (2004a).
- [19] Eyles, L.P., et al. MNRAS, (2005)
- [20] Mobasher, B., et al. ApJ, submitted (2005)
- [21] Kelson, D., PASP **115**, 688 (2003)
- [22] Kennicutt, R. ARAA **36**, 189 (1998)
- [23] Loeb, A., & Barkana, R. ARAA, **39**, 19 (2001)
- [24] Yan, H., et al. ApJ in press (astro-ph/0507673)